Journal of the Korean Ceramic Society
Vol. 42, No. 1, pp. 16~21, 2005.

Effect of Additive Composition on Mechanical Properties of Silicon Carbide Sintered with Aluminum Nitride and Erbium Oxide

Sung-Hee Lee and Young-Wook Kim†

Department of Materials Science and Engineering, The University of Seoul, Seoul 130-743, Korea
(Received November 15, 2004; Accepted December 4, 2004)

ABSTRACT

The effect of additive composition, using AlN and Er_2O_3 as sintering additives, on the mechanical properties of liquid-phase-sintered, and subsequently annealed SiC ceramics was investigated. The microstructures developed were quantitatively analyzed by image analysis. The average thickness of SiC grains increased with increasing the $Er_2O_3/(AlN + Er_2O_3)$ ratio in the additives whereas the aspect ratio decreased with increasing the ratio. The mechanical properties versus $Er_2O_3/(AlN + Er_2O_3)$ ratio curve had a maximum; i.e., there was a small composition range at which optimum mechanical properties were realized. The best results were obtained when the ratio ranged from 0.4 to 0.6. The flexural strength and fracture toughness of the SiC ceramics were 550~650 MPa and 5.5~6.5 MPa·$m^{1/2}$, respectively.

Key words : Silicon carbide, Mechanical properties, Aluminum nitride

1. Introduction

Interest in liquid-phase sintered SiC ceramics has grown continually over recent years because such materials are easier to process and seem to have superior mechanical properties than solid-state sintered SiC ceramics.[1-6] Typically, liquid-phase sintered SiC ceramics are densified by employing various mixtures of additives (e.g. Al_2O_3 and Y_2O_3) that, in combination with the surface oxide on the SiC powder particles, result in the formation of amorphous phases at grain boundaries. Various kinds of liquid-forming additives, such as Al_2O_3,[7] Al_2O_3-Y_2O_3,[8,9] Al_2O_3-Gd_2O_3,[10] Al_2O_3-Y_2O_3-CaO,[11] Al_2O_3-Y_2O_3-MgO,[12] Y_2O_3-AlN,[13] and Y-Mg-Si-Al-O-N glass,[14] have already been explored with respect to the liquid-phase sintering of SiC. The liquid phases formed during densification can provide a medium for the growth of platelet SiC grains. The growth of platelet grains is achieved via the $\beta \rightarrow \alpha$ phase transformation of SiC and/or accelerated solution-reprecipitation by seeding during liquid-phase sintering.[4,11] These platelet grains can act as a reinforcing phase that promotes crack bridging and deflection, and toughens the ceramics.[15] For this to occur, the platelet grains must remain intact as the crack front approaches and passes them. Furthermore, it must be easier for the crack front to deflect along a surface (typically a basal plane) of platelet grains than to cut through them.[14,15] This interfacial debonding of the platelet grains involves fracture either at the glass-SiC interface or within the glass phase near the interface.

In self-reinforced SiC ceramics, there are several observations that the composition of sintering additives and, hence, the grain boundary amorphous phase can significantly alter toughening processes.[16,17] Kim *et al.*[16] observed in self-reinforced SiC ceramics with almost same microstructures but different additive compositions in the $Y_3Al_5O_{12}$-SiO_2 system that one of the additive compositions showed a maximal toughness. Zhou *et al.*[17] also observed that the fracture toughness of SiC ceramics was strongly dependent on additive compositions in the Re_2O_3-Al_2O_3 system (Re = La, Nd, Y, Yb). Comparable effects were also observed in self-reinforced Si_3N_4 ceramics.[18-20] Therefore, manipulating the composition of the additives, and thus the glass chemistry, can play a significant role in the controlling of the crack propagation behavior.

Recently, a heat resistant SiC ceramic with improved high-temperature strength (~550 MPa at 1600°C) was fabricated using AlN and Er_2O_3 as sintering additives.[21] Moreover, the SiC ceramic with AlN and Er_2O_3 exhibited good oxidation resistance at 1300°C.[22] In this paper, the effect of additive composition on the room temperature mechanical properties of SiC ceramics was investigated for SiC ceramics sintered with AlN and Er_2O_3.

2. Experimental Procedure

Commercially available α-SiC (A-1 grade, Showa Denko, Tokyo, Japan), β-SiC (Ultrafine grade, Betarundum, Ibiden Co. Ltd., Ogaki, Japan), AlN (Grade F, Tokuyama Soda Co., Tokyo, Japan), and Er_2O_3 (99.9% pure, Shin-Etsu Chemical Co., Tokyo, Japan) were used as the starting powders. The mean particle sizes of the α- and β-SiC powders were 0.45

†Corresponding author : Young-Wook Kim
E-mail : ywkim@uos.ac.kr
Tel : +82-2-2210-2760 Fax : +82-2-2215-5863

and 0.27 μm, respectively, and the specific surface areas of each powder were 15 and 17.5 m^2/g, respectively.

Five batches of powder were mixed, each containing 90 vol% SiC and 10 vol% additives (see Table 1). To accelerate the development of a self-reinforced microstructure, we used a mixture comprised of 1 vol% α-SiC and 99 vol% β-SiC as the starting material. The relative content of Er_2O_3 in the additives of those batches was 0, 20, 40, 60, and 80 mol%. All individual batches were milled in ethanol for 24 h using SiC grinding balls. The milled slurry was dried, sieved, and hot-pressed at 1900°C for 1 h under a pressure of 25 MPa in N_2 atmosphere. The hot-pressed specimens were further annealed at 2000°C for 6 h with an applied pressure of 25 MPa.

The relative densities of the sintered and annealed specimens were determined by the Archimedes method using deionized water as the immersion medium. The hot-pressed and annealed specimens were cut, polished, and then etched by a CF_4 plasma containing 7.8% O_2. The microstructures were observed by Scanning Electron Microscopy (SEM). The SEM micrographs were quantitatively analyzed by image analysis, according to the procedure outlined in a previous study.[15] The thickness of each grain (t) was determined directly from the shortest grain dimension in its two-dimensional image; the apparent length of each grain (l) was obtained from the largest dimension. The mean value of the observed aspect ratio (l/t) was taken to be the average aspect ratio. A total of 900 to 1100 grains were used for the statistical analysis of each specimen. X-Ray Diffraction (XRD) using Cukα radiation was performed on ground powders for the annealed specimens.

For the strength measurements, bar-shaped specimens were ground to a size of 3 × 2.5 × 25 mm. The tensile surfaces of the bars were polished to a 1 μm diamond finish and the tensile edges beveled to avoid stress concentrations and large edge flaws caused by sectioning. Bend tests were performed at room temperature on five to seven specimens at each compositon, using a four-point method with an inner and outer span of 10 and 20 mm, respectively. The specimens were loaded at a constant crosshead speed of 0.5 mm/min. The fracture toughness was determined by measuring the crack lengths that were generated by a Vickers indenter.[23] The variation of fracture toughness with indentation load (R-curve-like behavior) was estimated by changing the indentation load over a range of 49 – 294 N, and the toughness values measured in the steady-state region are reported in this study.

3. Results and Discussion

Table 1 shows the densities of the annealed specimens. The theoretical densities of each specimen were calculated on the assumption that no chemical reactions occurred between SiC and the sintering additives. By hot-pressing and subsequently annealing with pressure, relative densities of >97% were achieved when the $Er_2O_3/(AlN + Er_2O_3)$ ratio ranged from 0.2 to 0.8 (SCER1-SCER4). During hot-pressing, $AlN\text{-}Er_2O_3$ additives react with SiO_2, which is always present on the surface of SiC particles, to form an Al-Er-Si-O-N oxynitride melt, and with increasing the temperature, an Al-Er-Si-O-C-N oxycarbonitride melt by dissolution of SiC.[24] The liquid phase promoted densification through liquid-phase-sintering.[21] A specimen without Er_2O_3 (SCER0) displayed relatively lower density (85.2%) than the other specimens because of a slow kinetic of solid-state material transport in the specimen. Present results indicate that $AlN\text{-}Er_2O_3$ liquid is an effective additive for the liquid-phase sintering of SiC ceramics.

Fig. 1 shows the typical microstructures of the sintered and annealed specimens. All specimens contain the same total amount of glass (10 vol%), and exhibit $Er_2O_3/(AlN + Er_2O_3)$ ratios ranging from 0.2 to 0.8. The microstructure of SCER0 is not shown because its extremely low density makes it difficult to polish the specimen for observing the microstructure. Core/rim structure in Fig. 1 indicates that grain growth has occurred through a solution-reprecipitation process.[25] The microstructure of SCER1-SCER3 consisted of elongated grains in 2-dimensional image (platelet grains in 3-dimension). In contrast, that of SCER4 consisted of mostly equiaxed grains. When the $Er_2O_3/(AlN + Er_2O_3)$ ratio was increased, the shape of the grains changed from elongated to equiaxed and the thickness of the grains increased. Transmission electron microscopy confirmed a thin (9 Å) residual amorphous film at two-grain boundaries in SCER2.[21]

The grain-thickness distribution of some selected specimens are illustrated in Fig. 2. SCER2 has a grain-thickness distribution that spans 0.25 to 7.94 μm. In contrast, SCER4 has a grain thickness-distribution of 0.40 to 9.89 μm. As shown in Fig. 3, the thickness increased as a result of

Table 1. Characteristics of the Sintered and Annealed Specimens

Specimen designation	Batch composition (wt%)	Relative density (%)	Crystalline phase	
			Major	Minor
SCER0	89.0% β-SiC + 0.9% α-SiC + 10.1% AlN	85.2	β-SiC	α-SiC
SCER1	82.5% β-SiC + 0.8% α-SiC + 5.0% AlN + 11.7% Er_2O_3	97.0	α-SiC	β-SiC
SCER2	79.6% β-SiC + 0.8% α-SiC + 2.7% AlN + 16.9% Er_2O_3	98.2	α-SiC	β-SiC
SCER3	78.0% β-SiC + 0.8% α-SiC + 1.4% AlN + 19.8% Er_2O_3	97.5	α-SiC, β-SiC	–
SCER4	76.9% β-SiC + 0.8% α-SiC + 0.6% AlN + 21.7% Er_2O_3	97.1	β-SiC	α-SiC

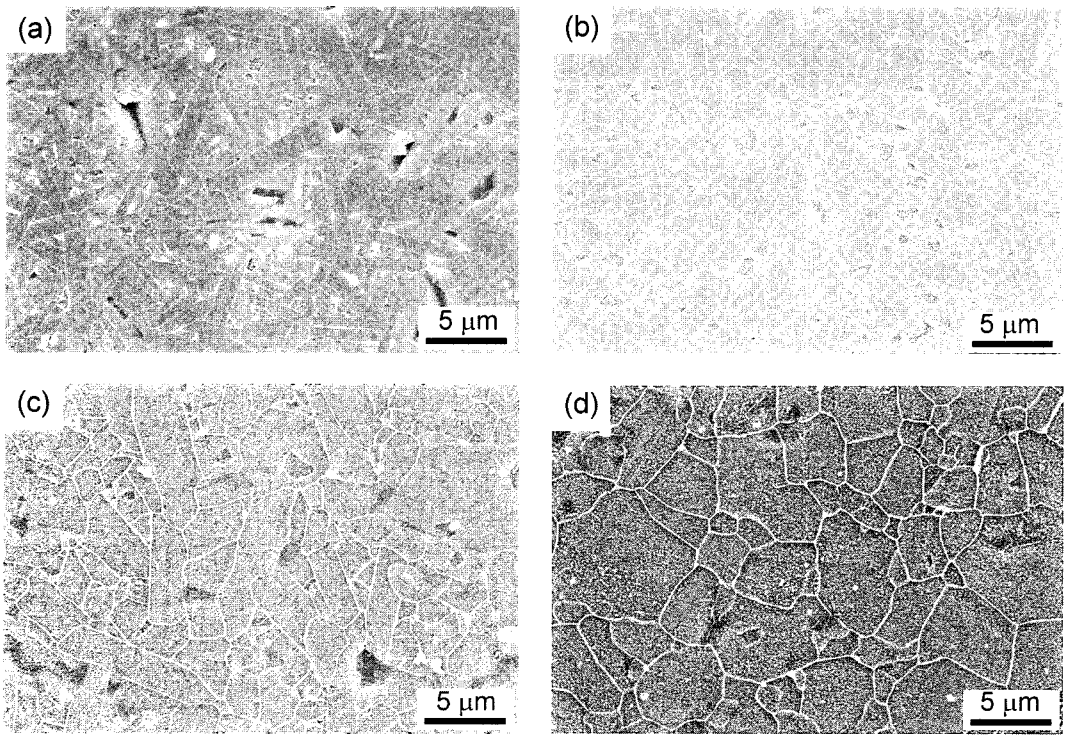

Fig. 1. Typical microstructures of SiC ceramics: (a) SCER1, (b) SCER2, (c) SCER3, and (d) SCER4 (refer to Table 1).

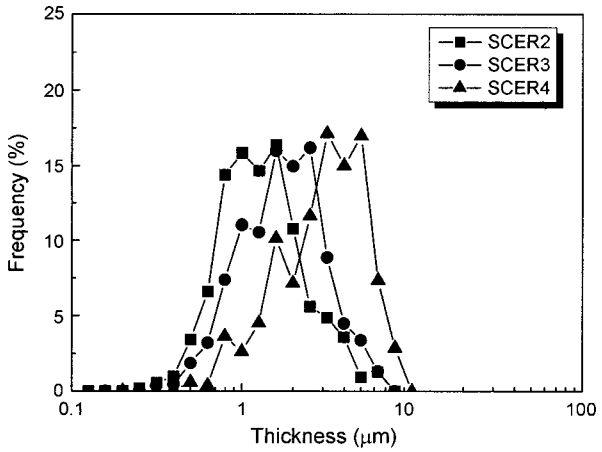

Fig. 2. Grain-thickness distributions of SCER2, SCER3, and SCER4 (refer to Table 1).

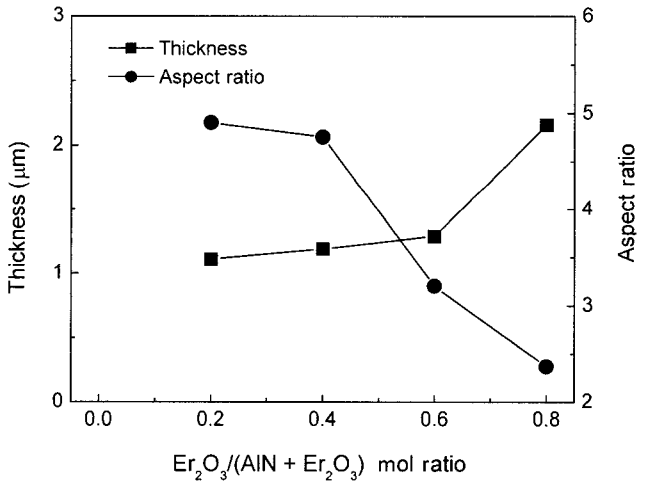

Fig. 3. Change of grain thickness and aspect ratio of SiC grains for the sintered and annealed SiC ceramics as a function of Er_2O_3/(AlN+Er_2O_3) mol ratio at constant 10 vol% additive content.

increasing the Er_2O_3/(AlN + Er_2O_3) ratio in the additives, whereas the aspect ratio decreased when the ratio was increased. Among the batches investigated herein, SCER1 had the maximum aspect ratio and SCER4 the maximum thickness. It is noteworthy that an increase of AlN content in the sintering additives increased the aspect ratio of SiC grains. Shinozaki[26] observed the presence of Al at the acute tip of elongated SiC grains sintered with Al_2O_3 by using analytical electron microscopy. Shinozakis work and the present results suggest that Al played an important role in the elongation process of SiC grains during sintering and/or annealing. Referring to the phase analysis in Table 1, the presence of both Al and the liquid phase accelerated the β→α phase transformation of SiC grains, thus yielding elongated grains with high aspect ratios.

Fig. 4 shows the variation of fracture toughness and strength as a function of the Er_2O_3/(AlN + Er_2O_3) ratio in the additives: i.e., each specimen had different intergranular film chemistry. All specimens had the same total amount of glass (10 vol%) with Er_2O_3/(AlN + Er_2O_3) ratios ranging from 0 to 0.8. The toughness of SCER0 couldn't be

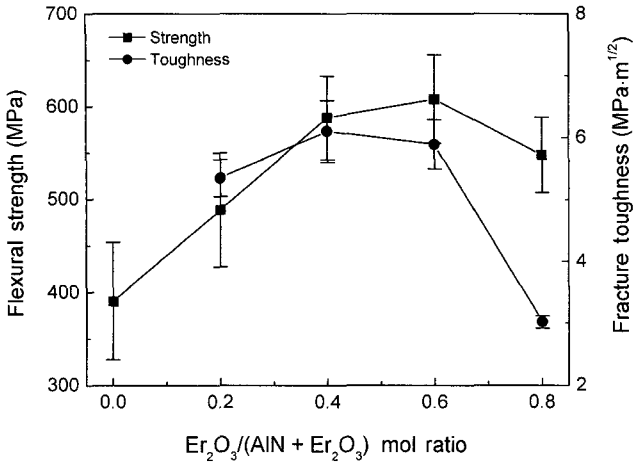

Fig. 4. Flexural strength and fracture toughness of the sintered and annealed SiC ceramics as a function of Er_2O_3/(AlN+Er_2O_3) mol ratio at constant 10 vol% additive content.

measured because of its low sintered density. The highest strength (608 ± 47 MPa) was obtained for the Er_2O_3/(AlN + Er_2O_3) ratio of 0.6 and the highest toughness (6.1 ± 0.5 MPa · $m^{1/2}$) for the ratio of 0.4. The initial addition of Er_2O_3 in the glass increased these properties, but at ratios spanning 0.4 to 0.6, there were maxima in both properties and beyond the ratio the properties decreased. The flexural strength and fracture toughness of the specimens with ratios ranging from 0.4 to 0.6 were 588~608 MPa and 5.9~6.1 MPa · $m^{1/2}$, respectively.

It is well documented that the mechanical properties of liquid-phase sintered SiC ceramics are strongly dependent on their microstructures. The fracture toughness of SiC ceramics increased in proportion to the square root of grain diameter as well as the aspect ratio of large grains in SiC ceramics sintered with Al_2O_3, Y_2O_3, and CaO as sintering additives.[27] The fracture toughness of SiC ceramics sintered with Al_2O_3 and Y_2O_3 was also observed to increase when the thickness of SiC grains increased.[28] However, the present results showed a different tendency. SCER1 has the largest aspect ratio (4.9), but lower fracture toughness than SCER2. SCER4 has thicker grains than SCER2, but lower toughness than SCER2. The dramatic increase in toughness from 3.0 MPa · $m^{1/2}$ (SCER4) to 6.1 MPa · $m^{1/2}$ (SCER2) and the measurable increase from 5.3 MPa · $m^{1/2}$ (SCER1) to 6.1 MPa · $m^{1/2}$ (SCER2) are difficult to explain on the basis of grain morphology alone. Thus, SiC morphology is not the primary factor affecting fracture toughness in the present results. Similar results have also been observed: (1) the mechanical properties of SiC ceramics sintered with $Y_3Al_5O_{12}$ and SiO_2 showed a maximum when the SiO_2/$Y_3Al_5O_{12}$ ratio was 0.5[16]; (2) the fracture toughness of SiC ceramics was strongly dependent on additive compositions in the Re_2O_3-Al_2O_3 system (Re = La, Nd, Y, Yb).[17]

As shown in Fig. 5, the fracture mode of SCER4 was mostly transgranular, whereas that of SCER2 was mostly

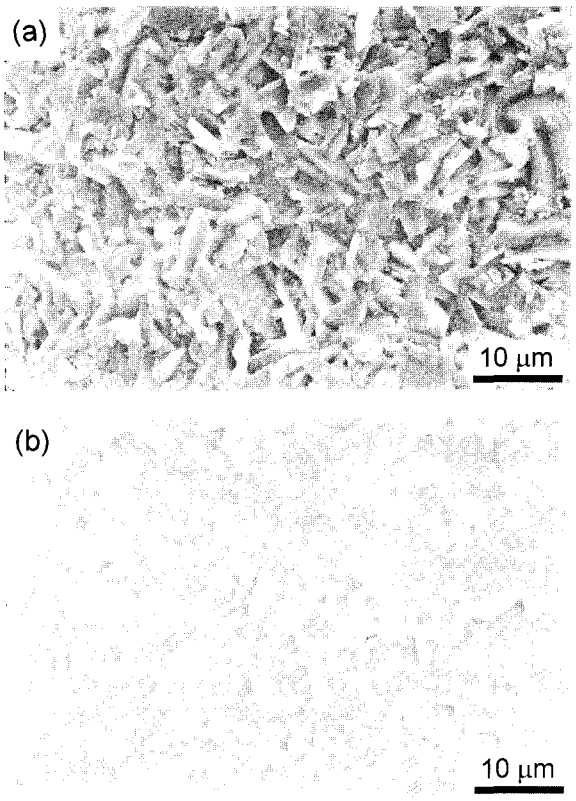

Fig. 5. SEM micrographs of fracture surfaces after bending test at room temperature: (a) SCER2 and (b) SCER4. Note the fracture surface in SCER2 is more tortuous than SCER4 and the tendency to form intergranular fracture is more apparent in SCER2.

intergranular. The more tortuous crack path in SCER2 may be due to an optimal interface strength, which affects crack propagation behavior, for intergranular fractures. Among the compositions investigated herein, the present results suggest that the interface strength of SCER2 is optimal for inducing intergranular factures. Thus, the interface strength of SiC ceramics can be controlled by manipulating glass chemistry, as reported for Si_3N_4.[19,20]

Generally, the introduction of large elongated grains into the microstructure has resulted in the decreased strength.[28,29] Our results showed that SCER2 has a smaller thickness of SiC grains, but a lower strength than SCER3. The critical flaw size (c) for specimens SCER1-SCER4 were calculated from the measured values of fracture toughness (K_{IC}) and strength (s) using the equation $K_{IC} = 1.35\ sc^{1/2}$, assuming semielliptical surface flaws and compared with the average length of grains in Table 2. As shown, the critical flaw size decreases with the increase of Er_2O_3 content in the additives. The calculated flaw sizes are much larger than the average length of grains for SCER1-SCER3, which indicates that only external flaws acted as fracture origins. Typical fracture origins in specimens SCER1-SCER3 were pores near or on the surface. In contrast, the calculated flaw size of SCER4 was only 3 times the average length of SiC grains, suggesting the possibility that intrinsic flaws acted as frac-

Table 2. Average Grain Length and Calculated Flaw Size of the Sintered and Annealed Specimens (Refer to Table 1)

Specimen	Average length of grains (μm)	Calculated flaw size (μm)
SCER1	5.4	66
SCER2	5.7	59
SCER3	4.1	52
SCER4	5.1	17

ture origins. From the calculated flaw sizes, SCER4 was expected to have higher strength than the others. But the average strength of SCER4 (548 MPa) was lower than that of SCER3 (608 MPa). Furthermore, the measurable increase in strength from 489 MPa (SCER1) to 608 MPa (SCER3) is difficult to explain on the basis of grain morphology alone, i.e., SiC morphology is not the primary factor affecting strength property. As shown in Fig. 4, the change in strength with the $Er_2O_3/(AlN + Er_2O_3)$ ratio is comparable to the relative change in toughness, demonstrating that toughness is a dominant factor in the improved strength at the ratio of 0.6.

The present results indicate that tailoring the intergranular phase chemistry, which is in turn controlled by the sintering additive composition, affects the mechanical properties of liquid-phase sintered SiC ceramics not only by directly modulating the intergranular film strength, but also through its influences on the development of the final microstructures.

4. Conclusions

Silicon carbide ceramics with Er_2O_3 and AlN as sintering additives with relative densities of >97% have been fabricated by hot-pressing and subsequent annealing with pressure when the $Er_2O_3/(AlN + Er_2O_3)$ ratio ranged from 0.2 to 0.8. An increase in the ratio, i.e., a large addition of Er_2O_3, led to an increase in grain thickness and to a decrease in aspect ratio of SiC grains. The mechanical properties were not only dependent on grain morphology but rather on sintering additive composition, i.e., the glass chemistry of an intergranular film. There was a small composition range, the $Er_2O_3/(AlN + Er_2O_3)$ ratios ranging from 0.4 to 0.6, at which optimal mechanical properties were realized. The flexural strength and fracture toughness of the specimens were 550~650 MPa and 5.5~6.5 MPa · $m^{1/2}$, respectively.

Acknowledgments

This work was supported by the Research Grant of the University of Seoul in 2003.

REFERENCES

1. S. Prochazka, "The Role of Boron and Carbon in the Sintering of Silicon Carbide," in Special Ceramics, Vol. 6, Ed. by P. Popper(Manchester: The British Ceramic Research Association, pp. 171-78, 1975.
2. R. A. Culter and T. B. Jackson, "Liquid Phase Sintered Silicon Carbide," pp. 309-18, in Ceramic Materials and Components for Engines, Proceedings of the Third International Symposium edited by V. J. Tennery. The American Ceramic Society, Westerville, OH, 1989.
3. Y. I. Lee and Y.-W. Kim, "Microstructure and Mechanical Properties of SiC-BN Composites with Oxynitride Glass," *J. Kor. Ceram. Soc.*, **40** [3] 229-33 (2003).
4. N. P. Padture, "In Situ-Toughened Silicon Carbide," *J. Am. Ceram. Soc.*, **77** 519-23 (1994).
5. D. Chen, M. E. Sixta, X. F. Zhang, L. C. De Jonghe, and R. O. Ritchie, "Role of the Grain-Boundary Phase on the Elevated-Temperature Strength, Toughness, Fatigue, and Creep Resistance of Silicon Carbide Sintered with Al, B, and C," *Acta Mater.*, **48** 4599-608 (2000).
6. G. Rixecker, I. Wiedmann, A. Rosinus, and F. Aldinger, "High-Temperature Effects in the Fracture Mechanical Behavior of Silicon Carbide Liquid-Phase Sintered with $AlN-Y_2O_3$ Additives," *J. Eur. Ceram. Soc.*, **21** 1013-19 (2001).
7. M. A. Mulla and V. D. Krstic, "Pressrueless Sintering of β-SiC with Al_2O_3 Additions," *J. Mater. Sci.*, **29**, 934-38 (1994).
8. S. H. Kim, Y.-W. Kim, J. Y. Yoon, and H. D. Kim, "Fabrication of Porous SiC Ceramics by Partial Sintering and their Properties," *J. Kor. Ceram. Soc.*, **41** [7] 541-47 (2004).
9. E. J. Winn and W. J. Clegg, "Role of the Powder Bed in the Densification of Silicon Carbide Sintered with Yttria and Alumina Additives," *J. Am. Ceram. Soc.*, **82** [12] 3466-536 (1999).
10. Z. Chen, "Effects of Gadolinia and Alumina Addition on the Densification and Toughening of Silicon Carbide," *J. Am. Ceram. Soc.*, **79**, 530-32 (1996).
11. Y. J. Jin, Y.-W. Kim, and M. Mitomo, "Effect of Large Seeds Addition on Microstructural Development of SiC Sintered with Oxynitride Glass," *J. Mater. Sci. Lett.*, **21** 1015-17 (2002).
12. D. Foster and D. P. Thompson, "The Use of MgO as a Densification Aid for α-SiC," *J. Eur. Ceram. Soc.*, **19** 2823-31 (1999).
13. M. Keppeler, H. G. Reichert, J. M. Broadley, G. Thurn, I. Weidmann, and F. Aldinger, "High Temperature Mechanical Behaviour of Liquid Phase Sintered Silicon Carbide," *J. Europ. Ceram. Soc.*, **18** [5] 521-26 (1998).
14. S. H. Kim, Y.-W. Kim, and M. Mitomo, "Microstructure and Fracture Toughness of Liquid-Phase-Sintered β-SiC Containing β-SiC Whiskers as Seeds," *J. Mater. Sci.*, **38** 1117-21 (2003).
15. S. G. Lee, Y.-W. Kim, and M. Mitomo, "Relationship between Microstructure and Fracture Toughness of Toughened Silicon Carbide," *J. Am. Ceram. Soc.*, **84** 1347-53 (2001).
16. J. Y. Kim, Y.-W. Kim, M. Mitomo, G. D. Zhan, and J. G. Lee, "Microstructure and Mechanical Properties of α-SiC Sintered with Yttrium-Garnet and Silica," *J. Am. Ceram. Soc.*, **82** 441-44 (1999).
17. Y. Zhou, K. Hirao, Y. Yamauchi, and S. Kanzaki, "Tailoring the Mechanical Properties of Silicon Carbide Ceramics by Modification of the Intergranular Phase Chemistry and Microstructure," *J. Eur. Ceram. Soc.*, **22** 2689-96 (2002).
18. Y. Tajima, "Developemnt of High Performance Silicon

Nitride Ceramics and their Applications," *Mat. Res. Soc. Proc.*, **287** 189-96 (1993).
19. P. F. Becher, E. Y. Sun, C.-H. Hsueh, K. B. Alexander, S.-L. Hwang, S. B. Waters, and C. G. Westmoreland, "Debonding of Interfaces between Beta-Silicon Nitride Whiskers and Si-Al-Y Oxynitride Glasses," *Acta Mater.*, **10** 3881-93 (1996).
20. E. Y. Sun, P. F. Becher, K. P. Plucknett, C.-H. Hsuch, K. B. Alexander, S. B. Waters, K. Hirao, and M. E. Brito, "Microstructural Design of Silicon Nitride with Improved Fracture Toughness: II, Effects of Yttria and Alumina Additives," *J. Am. Ceram. Soc.*, **81** [11] 2831-71 (1998).
21. Y.-W. Kim, M. Mitomo, and T. Nishimura, "Heat-Resistant SiC with Aluminum Nitride and Erbium Oxide," *J. Am. Ceram. Soc.*, **84** 2060-64 (2001).
22. S. Guo, N. Hirosaki, H. Tanaka, Y. Yamamoto, and T. Nishimura, "Oxidation Behavior of Liquid-Phase Sintered SiC with AlN and Er_2O_3 Additives between 1200°C and 1400°C," *J. Eur. Ceram. Soc.*, **23** [12] 2023-29 (2003).
23. G. R. Anstis, P. Chantikul, B. R. Lawn, and D. B. Marshall, "A Critical Evalution of Indentation Techniques for Measuring Fracture Toughness," *J. Am. Ceram. Soc.*, **64** 533-38 (1981).
24. Y.-W. Kim, K. Ando, and M. C. Chu, "Crack-Healing Behavior of Liquid-Phase-Sintered Silicon Carbide Ceramics," *J. Am. Ceram. Soc.*, **86**, 465-70 (2003).
25. L. S. Sigl and H. J. Kleebe, "Core/Rim Structure of Liquid-Phase-Sintered Silicon Carbide," *J. Am. Ceram. Soc.*, **76** 773-76 (1993).
26. S. S. Shinozaki, "Unique Microstructural Development in SiC Materials with High Fracture Toughness," *MRS Bull.*, **20** 42-5 (1995).
27. Y.-W. Kim, M. Mitomo, and H. Hirotsuru, "Microstructural Development of Silicon Carbide Containing Large Seed Grains," *J. Am. Ceram. Soc.*, **80** 99-105 (1997).
28. Y.-W. Kim, M. Mitomo, H. Emoto, and J. G. Lee, "Effect of Initial α-Phase Content on Microstructure and Mechanical Properties of Sintered Silicon Carbide," *J. Am. Ceram. Soc.*, **81** 3136-40 (1998).
29. J. Y. Kim, Y.-W. Kim, J. G. Lee, and K. S. Cho, "Effect of Annealing on Mechanical Properties of Self-Reinforced Alpha-Silicon Carbide," *J. Mater. Sci.*, **34** 2325-30 (1999).